STRUCTURE OF LOW-DENSITY SUPERSONIC JET

V. I. Nemchenko and N. I. Yushchenkova

The use of supersonic jets to obtain intense molecular beams and high-velocity, low-temperature plasma streams has stimulated the development of experimental and theoretical studies on the structure of underexpanded supersonic jets. The structure of the initial segment of the supersonic underexpanded jet is characterized by the position, dimensions, and shape of the closing shock.

Theoretical estimates and some experimental data are presented in [1-7] on the shape of the catenary shock and on the location and diameter of the central shock. However, most of the studies correspond to ideal gas flow conditions in the continuum regime.

With reduction of the jet density we would expect a change of the flow structure, since the transport processes, whose role increases with decreasing density, have a significant effect on catenary shock formation and the jet boundary.

The results presented in this paper from an experimental study of the structure of a supersonic air jet for different discharge conditions $10 \leq n \leq 10^4$, $1.15 \leq M_a \leq 3.3$, $10^{-4} \leq K_* = \lambda_*/d_* \leq 10^{-3}$, where M_a is is the Mach number at the nozzle exit, λ_* is the molecular mean free path at the nozzle critical section, d_* is the nozzle critical section diameter, and n is the ratio of the nozzle exit pressure to the ambient pressure, make it possible to identify the influence of high pressure ratios n, high Mach number M_a, and flow rarefaction on the structure of the supersonic underexpanded jet. The Knudsen number K_* and the parameter $C = K_* \sqrt{n}$ are also used to characterize the flow rarefaction.

1. The experiments were conducted in the low-density wind tunnel described in [8]. The working gas was air, preheated to ~600°K to prevent condensation during adiabatic expansion [9]. The gas jet discharged through a supersonic conical nozzle into a low-pressure chamber. The nozzle dimensions and jet discharge conditions are shown in Table 1, where in column d the upper numeral corresponds to the nozzle throat diameter and the lower numeral is the nozzle exit diameter; ξ_0 is the nozzle half-angle; in the column M the upper numeral is the Mach number M_a' at the nozzle exit, calculated for isentropic expansion of the gas, and the lower numeral is the nozzle exit Mach number, obtained from measurements of the total pressure p_0'; and p_0 is the adiabatic flow stagnation pressure, in mm Hg.

The following parameters were measured in the experiments: pressure p_0 and temperature T_0 in the adiabatically decelerated flow, the total pressure p_0', and the vacuum chamber pressure p_1. A Pitot tube of 0.8-mm diam. was used to measure the total pressure. The viscous corrections were introduced in accordance with the technique presented in [8]. The results of the p_0, T_0 measurements were used to calculate

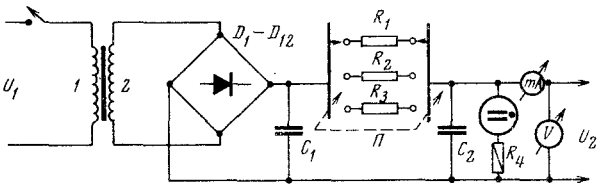

Fig. 1. Discharge gap power supply circuit.

Moscow. Translated from Zhurnal Prikladnoi Mekhaniki i Tekhnicheskoi Fiziki, Vol. 10, No. 6, pp. 110-115, November-December, 1969. Original article submitted June 15, 1967.

TABLE 1

d	ξ_0	M	p_0	K_*	n
1 1.01	55′	1.14	700 500 300	$2.14\cdot10^{-4}$ $3.01\cdot10^{-4}$ $5.01\cdot10^{-4}$	100—8000
1.85 3	6°12′	2.5 2.23—2.27	700 500 300 150 50	$1.16\cdot10^{-4}$ $1.62\cdot10^{-4}$ $2.7\cdot10^{-4}$ $5.4\cdot10^{-4}$ $1.62\cdot10^{-4}$	17—785
1.85 3.35	7°57′	2.75 2.5	700 500 300 150	$1.16\cdot10^{-4}$ $1.62\cdot10^{-4}$ $2.7\cdot10^{-4}$ $5.4\cdot10^{-4}$	37—1000
1.85 3.83	10°05′	3 2,8	700 500 300	$1.16\cdot10^{-4}$ $1.62\cdot10^{-4}$ $2.7\cdot10^{-4}$	20—500
1.5 4.4	10°20′	3.5 3.4	700 500 300	$1.43\cdot10^{-4}$ $2.1\cdot10^{-4}$ $3.34\cdot10^{-4}$	24—227

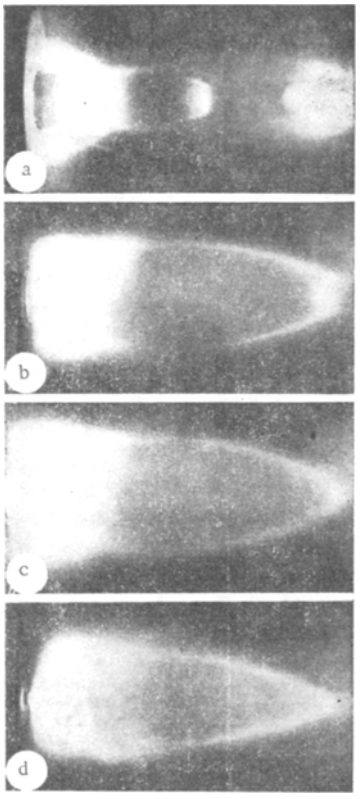

Fig. 2. Results of glow discharge jet visualization. For the case $M_a = 2.8$ $K_* \approx 1.62 \cdot 10^{-4}$, (a), (b), and (c) correspond to the value $n = 56$, 176, 185; for the case $M_a \approx 3.3$ $K_* \approx 1.43 \cdot 10^{-4}$, (d) corresponds to $n = 87$.

the flow parameters at the nozzle throat, and the measured values of p_0', p_0 were used to calculate the parameters at the nozzle exit and in the jet.

The pressure measurements in the range from 10^{-3} to 10^{-1} mm Hg were made using the LT-2 thermocouple manometer, which was calibrated against compression manometers; the higher pressures from 10^{-2} to 10 mm Hg were measured using the VR-3 radioactive manometer, also calibrated against compression manometers. The pressure measurement in the range from 1 to 700 mm Hg was made using oil and mercury U-tube manometers. The relative pressure measurement error in the range from 10^{-3} to 1 mm Hg did not exceed 3%, and in the range from 1 to 700 mm Hg the error did not exceed 1%.

To study the structure of the initial segment of the supersonic underexpanded jet at low flow densities, when the schlieren technique cannot be used, we used the glow discharge flow visualization method which is widely used in studying supersonic gas flow past bodies. For example, studies of supersonic rarefied gas flow past a flat plate with a sharp leading edge, made in [10] with the aid of the glow discharge technique, and studies using the schlieren method, thin-film sensors, hot-wire anemometers, and total head tubes have shown that the shock wave shapes obtained by the various methods are the same.

For visualization of the jet flow field we used a molybdenum rod reinforced with quartz as the discharge gap anode, and the nozzle itself, which was thermostatted, as the cathode. The discharge gap power supply circuit is shown in Fig. 1, where D_1, ..., D_{12} are the rectifying bridge diodes, and U_1, U_2 are the voltages at the input and output of the rectifier. The voltage U_1 was varied by the autotransformer from 10 to 250 V. For the concrete flow discharge conditions the discharge gap current I and the voltage drop V across the gap were selected experimentally in the ranges $0.5 \leq I \leq 40$ mA, $300 \leq V \leq 700$ V. The power put into the discharge gap did not exceed 20 W.

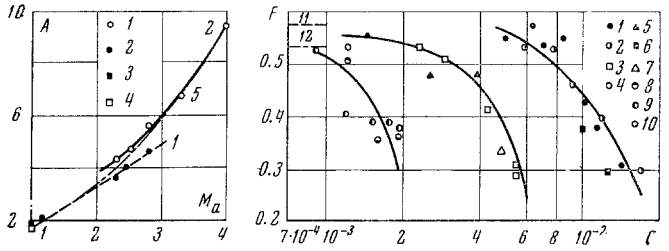

Fig. 3. a) Proportionality coefficients A and A_1 (2.1) of nozzle exit Mach number; b) values of the coefficient f for different M_a and $K_* \sqrt{n}$.

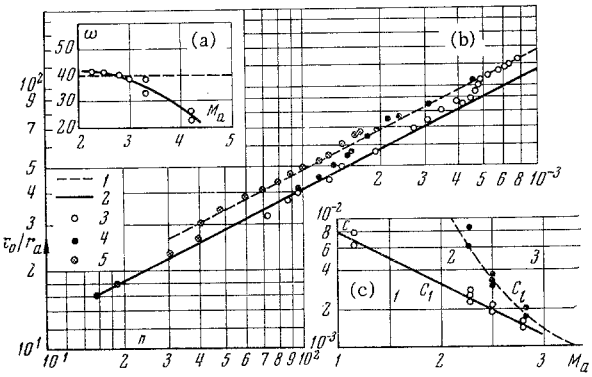

Fig. 4. a) Catenary shock incidence angle at the jet axis as a function of nozzle exit Mach number M_a; b) transition of central compression shock into an x-shock for $M_a = 2.5$ and different K_* with increase of the pressure ratio n; c) region of existence of different types of shock wave configurations near the jet axis: 1) region of existence of central compression shock; 2) region of transition of central compression shock into an x-shock; 3) region of existence of the x-shock.

TABLE 2

M_a	D/x_0	D_0/x_0	C
1.15	0.60	0.54	$2.8 \cdot 10^{-3}$—$7 \cdot 10^{-3}$
2.27	0.53	0.41	$1.2 \cdot 10^{-3}$—$1.7 \cdot 10^{-3}$
2.5	0.46	0.27	$1.4 \cdot 10^{-3}$—$1.7 \cdot 10^{-3}$
2.8	0.39	0.22	$1.1 \cdot 10^{-3}$—$2.0 \cdot 10^{-3}$
3.3	0.28		10^{-4}—$2.3 \cdot 10^{-3}$

Total pressure distribution measurements made along the jet axis with and without the discharge showed no influence of the discharge on the gas flow for $I < 40$ mA. Langmuir probe data showed that the free electron concentration in the jet did not exceed 10^8-10^9 cm^{-3}, which corresponds to a gas ionization degree of 10^{-6}. For an ionization degree less than 10^{-3}-10^{-4}, the influence of the discharge on the gasdynamic parameter field in the jet can be neglected [11], which makes it possible to use the glow discharge flow visualization technique to study the geometry and location of the shock waves occurring in the case of supersonic underexpanded jet discharge.

2. The jet photographs obtained (see, for example, Fig. 2a, b, c, d) made it possible to determine the geometry of the closing shock in the supersonic underexpanded air jet for different exit conditions; x_0 is the distance to the closing shock along the jet axis; D is the maximal diameter of the catenary compression shock; D_0 is the diameter of the central shock; and α is the angle at the triple point between the incident shock wave and the axial direction. The results of the study show that for high flow densities $K_* \sqrt{n} < 10^{-3}$ and $\gamma = \text{const}$, when the rarefaction influence is not significant, the ratios D/x_0, D_0/x_0 (Table 2) will be functions of the Mach number at the nozzle exit and will not depend on n, which characterizes self-similarity of the jet structure. A similar result was obtained in [1] by the schlieren technique for a jet with $M_a \approx 1$.

The position of the central compression shock is defined by a linear function of $\sqrt{n}$:

$$x_0/r_a = A\sqrt{n} \tag{2.1}$$

where r_a is the radius of the nozzle exit section, and A is a coefficient of proportionality, defined by the empirical relation

$$A \approx 1.38\sqrt{\gamma}M_a \tag{2.2}$$

suggested in [4]. In (2.2) γ is the specific heat ratio. The values of the coefficients A (points 2 in Fig. 3a), obtained as a result of analysis of the photographs of the jets visualized in the glow discharge, agree well with Eq. (2.2) and the results of experiments of other authors [1, 2], obtained by the schlieren technique for high flow densities (points 3 and 4 in Fig. 3a) up to some limiting Mach number M_{al}.

The results of the central compression shock diameter measurements show that for high stream densities and $M_a < M_{al}$ the central compression shock diameter is a function of $\sqrt{n}$

$$D_0/d_a = F\sqrt{n} \tag{2.3}$$

In the nozzle exit Mach number range $1.1 \leq M_a \leq 2.8$ the coefficient of proportionality F depends very little on M_a, and for approximate calculations it can be taken equal to 0.5 for $n > 20$. The values of the coefficient F are shown in Fig. 3b, where the points 1, ..., 10 correspond to the following parameter combinations (M_a, K*): 1 (1.15, 2.14, 10^{-4}), 2 (1.15, $3 \cdot 10^{-4}$), 3 (1.15, $5 \cdot 10^{-4}$), 4 (2.27, $1.16 \cdot 10^{-4}$), 5 (2.27, $1.62 \cdot 10^{-4}$), 6 (2.27, 10^{-4}), 7 (2.27, $5.4 \cdot 10^{-4}$), 8 (2.8, $1.16 \cdot 10^{-4}$), 9 (2.8, $1.62 \cdot 10^{-4}$), 10 (2.8, $2.7 \cdot 10^{-4}$). The results of a study of the central compression shock diameter (curves 11 and 12 in Fig. 3b), obtained by the schlieren method and published in [1] and [2], are in good agreement with the glow discharge jet visualization data for small values of $K_*\sqrt{n}$.

Increase of the nozzle exit Mach number M_a above some limiting value $M_{al} = f(K_*, n)$ leads to transition of irregular reflection of the catenary compression shock into regular reflection (Fig. 2d). In this case the catenary shock incidence angle ω (Fig. 4a) becomes less than the limiting value

$$\omega_l = \arcsin\frac{1}{\gamma} \text{ [12]}$$

Figure 4a shows the experimental data on the magnitude of the incidence angle on the jet axis, corresponding to the values $M_1 > 10$ and $K_*\sqrt{n} \approx 10^{-3}$. The transition from one type of reflection to the other at high stream densities takes place practically instantaneously and is accompanied by an abrupt reduction of the central shock diameter and increase of the distance from the nozzle exit to the point of intersection of the closing shock with the jet axis. The location of the x-shock for $M_a > M_{al}$ is determined by a relation similar to (2.1) but with a different proportionality coefficient (curve 2 and points 1 in Fig. 3a)

$$A_1 = \sqrt{\gamma}M_a^{3/2} \tag{2.4}$$

The results of the calculation of A (curve 5 in Fig. 3a) using the approximation theory of [13] agree well with the experimental data for $M_a \gg M_{al}$ and $M_a \ll M_{al}$ and high stream densities; this agreement breaks down in the transition region.

As the jet density decreases for $M_a < M_{al}$, either as a result of pressure reduction in the adiabatically decelerated flow or as a result of the marked expansion for the high pressure ratios n, we observe a change of the geometric chracteristics of the curved and central compression shocks, which shows up primarily in a reduction of the diameter of the central compression shock shown in Fig. 2a, b. For fixed values of K_* the beginning of the deviation of the ratio D_0/d_a from the value characteristic for ideal gas flow depends on M_a and n. The higher the Mach number for the same values of K_*, the earlier the deviation of D_0/d_0 from the values defined by (2.3) begins.

The parameter C [13] was used to correlate the results obtained on the effect of rarefaction on the flow in the central shock region.

The results of measurements of the dimensionless diameter of the central compression shock are shown in Fig. 3b, where M_a is the parameter. With increase of the rarefaction for $c > c_1 = f(M_a, \gamma)$ there is a gradual increase of the central shock distance from the nozzle exit along with the reduction of its diameter. Figure 4b shows the location of the central compression shock as a function of n for $M_a = 2.5$ and three values of K_*: 3 ($1.62 \cdot 10^{-4}$), 4 ($2.7 \cdot 10^{-4}$), 5 ($5.4 \cdot 10^{-4}$). Thus, increase of $C > C_1$ leads to transition

of the central shock, whose location is defined by (2.1) and (2.2) (curve 2 in Fig. 4b), into an x-shock (Fig. 2b, c), whose position is defined by (2.1) and (2.4) (curve 1 in Fig. 4b).

The region of transition of the central compression shock into the x-shock is shown in Fig. 4c in the coordinates M_a and C. With increase of M_a the transition region narrows, and for $M_a \approx 3.3$ or more under the experimental conditions there is regular reflection of the catenary shock from the jet axis, as shown in Fig. 2d. Characteristic for the central shock configuration in the transition region will be upstream convexity (inversion), as shown in Fig. 2b. For $1.2 \leq M_a < 3.3$ and values of $C < C_l$, there is irregular supersonic reflection of the shock with formation of a central compression shock. For $2.25 \leq M_a < 3.3$ and $C \approx C_l$ the central compression shock degenerates into an x-shock. The reduction of the central shock for $C > C_1$ and its degeneration into an x-shock for $C \approx C_l$ and fixed oblique shock incidence angle at the jet axis, whose value is close to the limiting value (Fig. 4a), can be explained by the reduction of the incident shock wave intensity owing to the influence of dissipative processes.

These results show that both the nozzle exit Mach number, which defines the catenary shock configuration, and the flow rarefaction affect the flow formation in the central compression shock region. Increase of the rarefaction for $C > C_l$ will lead to thickening and smearing of the curved compression shocks and reduction of the incident shock wave intensity in comparison with the ideal values. The dependence of C_1 and C_l on M_a for $\gamma = 1.4$ is shown in Fig. 4c.

LITERATURE CITED

1. S. Crist, P. M. Shermann, and R. D. Glass, "Study of the highly underexpanded sonic jet," AIAA Journal, vol. 4, no. 1, 1966.
2. E. S. Love, C. E. Grigsby, L. P. Lee, and M. I. Woodling, "Experimental and theoretical studies of axisymmetric free jets," NASA, TRR-6, 1959.
3. K. Bier and B. Schmidt, "Zur Form der Verdichtungs – stobe in Frei Expandierenden Gasstonien." Z. Angew. Phys., vol. 13, no. 11, 1961.
4. C. H. Lewis, Jr., and D. J. Carlson, "Normal shock location in underexpanded gas and gas-particle jets," AIAA Journal, vol. 2, no. 4, 1964.
5. N. I. Yushchenkova, V. I. Nemchenko, and S. A. Lyzhnikova, "Effect of elementary process kinetics on ionization of supersonic low-temperature plasma jet," collection: Low-Temperature Plasma [in Russian], Mir, Moscow, 1967.
6. I. P. Ginzburg, Aerogasdynamics [in Russian], Vysshaya shkola, Moscow, 1966.
7. T. G. Volkonskaya, "Caculation of supersonic axisymmetric jets," collection: Numerical Methods in Gasdynamics [in Russian], Izd-vo MGU, Moscow, 1963.
8. S. I. Kosterin, N. I. Yushchenkova, N. T. Belova, and B. D. Kamaev, "Study of effect of supersonic flow rarefaction on indications of total pressure probe," Inzh.-fiz. zh., vol. 5, no. 12, 1962.
9. F. L. Daum, "Air condensation in a hypersonic wind tunnel," AIAA Journal, vol. 1, no. 5, 1963.
10. W. J. McCroskey and J. G. McDougall, "Shock wave shapes on a sharp flat plate in rarefied hypersonic flow," AIAA Journal, vol. 4, no. 1, 1966.
11. V. M. Korovin, "Possible simplifications of the equations of a two-temperature partially ionized plasma," PMTF [Journal of Applied Mechanics and Technical Physics], vol. 6, no. 6, 1965.
12. Fundamentals of Gasdynamics [Russian translation], Izd-vo inostr. lit., Moscow, 1963.
13. N. I. Yushchenkova, B. D Kamaev, S. A. Lyzhnikova, and V. I. Nemchenko, "Structure and parameters of supersonic low-temperature plasma jet and transport phenomena in jets," collection: Thermophysical Properties of Liquids and Gases at High Temperatures and Plasma, Vol. 2, [in Russian]. Izd-vo Komiteta standartov, mer i izmer. priborov, Moscow, 1969.